LHCB 95-3, LHCC 95-3
Geneva, 16 November 1995

Replies to the Physics Questions

The LHC-B Collaboration

1 The angle α

1.1 Necessary Formalism

The decay time dependent CP asymmetry for the $\mathrm{B_d} \to \pi^+\pi^-$ decays is given by

$$A_{\mathrm{CP}}(t) = \frac{N_{+-}(t) - \overline{N}_{+-}(t)}{N_{+-}(t) + \overline{N}_{+-}(t)}$$

where $N_{+-}(t)$ and $\overline{N}_{+-}(t)$ are the time dependent decay rates for the initially pure B^0 and $\overline{\mathrm{B}}^0$ into $\pi^+\pi^-$. $A_{\mathrm{CP}}(t)$ can be parameterised as

$$A_{\mathrm{CP}}(t) = a \cos \Delta m\, t + b \sin \Delta m\, t \tag{1}$$

where Δm is the mass difference between the two mass eigenstates of the $\mathrm{B_d}$-meson. The parameters a and b are related to the tree and penguin decay amplitudes, denoted by T and P respectively, as

$$a = 2 \left| \frac{P}{T} \right| \sin(\delta_{\mathrm{P}} - \delta_{\mathrm{T}}) \sin \alpha$$

and

$$b = -\sin 2\alpha - 2 \left| \frac{P}{T} \right| \cos(\delta_{\mathrm{P}} - \delta_{\mathrm{T}}) \sin \alpha \cos 2\alpha$$

where δ_{T} and δ_{P} are the phases introduced by the strong interactions and α is one of the angles of the unitarity triangle. (An approximation has been made that the contribution from the penguin diagram is much smaller than that from the tree diagram.) The ratio $|P/T|$ can be estimated to be ≈ 0.2 from the relation $Br(\mathrm{B_d} \to \pi^+\pi^-) \approx Br(\mathrm{B_d} \to \mathrm{K}^\pm\pi^\mp)$ observed by the CLEO collaboration.

If there is no contribution from the penguin diagram, i.e. $P = 0$, or the penguin and tree diagrams have the same strong interaction phases, i.e. $\delta_{\mathrm{P}} = \delta_{\mathrm{T}}$, we have $a = 0$.

1.2 Effects of the penguin diagram

In order to visualise the effect of the penguin diagram on the CP asymmetry, a and b are plotted as a function of α in figure 1. The range of α is restricted to the allowed interval of 0° to 180° and the value of $|P/T|$ is assumed to be 0.2 with $\delta_{\rm P} - \delta_{\rm T} = 10°$, 30° and 50°. Note that the term proportional to a varies as $\sin\alpha$, whereas the term proportional to b varies as $\sin 2\alpha$.

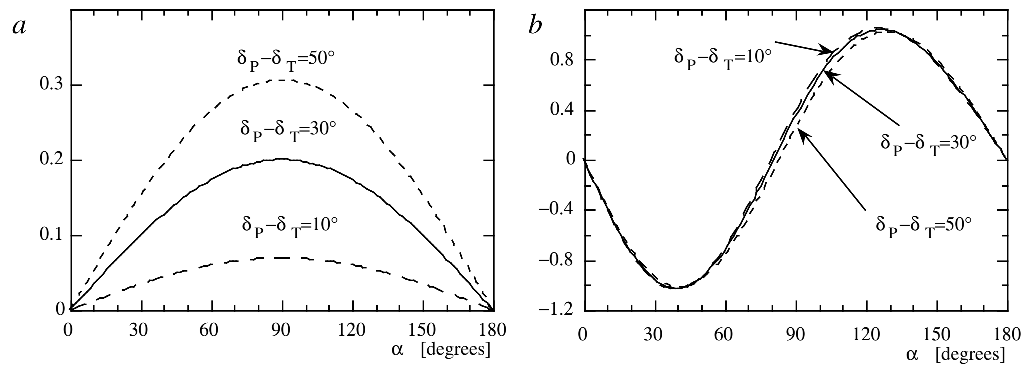

Figure 1: The parameters a and b as a function of α for $|P/T| = 0.2$ and $\delta_{\rm P} - \delta_{\rm T} = 10°$, 30° and 50°.

In table 1 values of a and b for $|P/T| = 0.2$, $\delta_{\rm P} - \delta_{\rm T} = 30°$ and $\alpha = 70°$, 80°, 90°, 100° and 110° are summarised.

Table 1: Values of a and b for $\alpha = 70°$, 80°, 90°, 100° and 110°, where a and b are obtained assuming $|P/T| = 0.2$ and $\delta_{\rm P} - \delta_{\rm T} = 30°$.

α	70°	80°	90°	100°	110°
a	0.188	0.197	0.200	0.197	0.188
b	−0.393	−0.021	0.346	0.663	0.892

1.3 Penguin diagram and other decay modes

Similarly to $\rm B_d \to \pi^+\pi^-$, the decay $\rm B_d \to \pi^0\pi^0$ proceeds through both the tree and penguin diagrams. However, the tree diagram contributing to the $\rm B_d \to \pi^+\pi^-$ decay is not identical to that contributing to the $\rm B_d \to \pi^0\pi^0$ decay. The former is colour allowed and the latter is colour suppressed (see figure 2). Due to this reason, the branching fraction for $\rm B_d \to \pi^0\pi^0$ is expected to be $\sim$10 times smaller than that for $\rm B_d \to \pi^+\pi^-$ making the detection of this decay channel very difficult. Also, the $\rm B_d \to \pi^0\pi^0$ decay alone does not provide direct information to estimate the size of the penguin diagram for the $\rm B_d \to \pi^+\pi^-$ decay.

Both tree diagrams contribute to the $\rm B^\pm \to \pi^\pm\pi^0$ decays and no penguin diagram is present in this decay mode. Thus, if all the three decay modes, $\rm B_d \to \pi^+\pi^-$, $\rm B_d \to \pi^0\pi^0$ and $\rm B^\pm \to \pi^\pm\pi^0$ are studied, the effect of the penguin diagram can be experimentally determined.

The branching fractions $Br(\rm B_d \to \pi^+\pi^-)$, $Br(\rm B_d \to \pi^0\pi^0)$ and $Br(\rm B^\pm \to \pi^\pm\pi^0)$ will be measured by CLEO, BaBar and BELLE, where the reconstruction of B-meson decay final states with π^0 is possible. One can therefore hope that the amplitude ratio $|P/T|$ will be determined with an accuracy of ±10% by the time of the LHC-B experiment.

The decay $\rm B_d \to K^\pm\pi^\mp$ is generated by both the penguin and colour allowed quark diagrams. The contribution to the decay from the penguin diagram is expected be larger than that from the tree diagram.

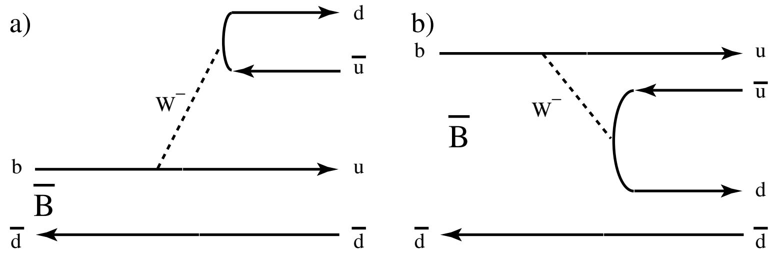

Figure 2: Tree diagrams contribution: (a) for $B_d \to \pi^+\pi^-$ and (b) for $B_d \to \pi^0\pi^0$.

The branching fraction of this decay mode will also be well measured by 2004 giving additional information on the penguin diagram. Note that $Br(B_d \to K^\pm\pi^\mp)$ can also be measured with very high statistics using the LHC-B detector .

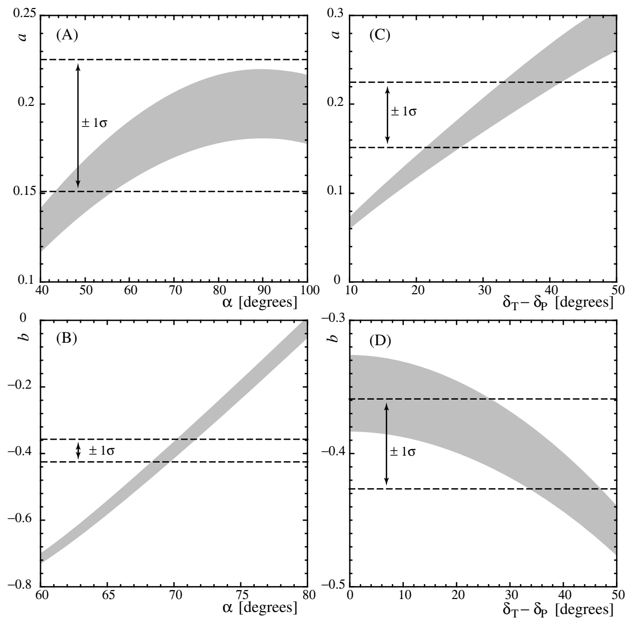

Figure 3: Expected measurement errors on a and b for the LHC-B experiment with one year of data taking are indicated by the dashed lines. The central values of a and b are for $|P/T| = 0.2$, $\delta_P - \delta_T = 30°$ and $\alpha = 70°$. The phenomenologically expected values of a and b are shown with the shaded band illustrating the effect of changing the value of $|P/T|$ by $\pm 10\%$ as a function of α assuming $\delta_P - \delta_T = 30°$ for (A) and (B) and as a function of $\delta_P - \delta_T$ assuming $\alpha = 70°$ for (C) and (D).

1.4 Sensitivity of LHC-B

The sensitivity of the LHC-B experiment to α in the presence of penguin diagram is illustrated in figure 3 where the expected experimental errors on a and b after one year data taking with the LHC-B detector are shown by the dashed lines. It is assumed that $|P/T| = 0.2$, $\delta_P - \delta_T = 30°$ and $\alpha = 70°$. For (A) and (B), the figures also show the phenomenologically expected values of a and b for $|P/T| = 0.20 \pm 0.02$ and $\delta_P - \delta_T = 30°$ as a function of α where the shaded bands indicate the effect of changing the value of $|P/T|$ by $\pm 10\%$. They demonstrate that α is mainly determined by the parameter b. In figures (C) and

(D), the phenomenologically expected values of a and b for $|P/T| = 0.20 \pm 0.02$ and $\alpha = 70°$ are shown as a function of $\delta_P - \delta_T$ where again the shaded bands indicate the effect of changing the value of $|P/T|$ by $\pm 10\%$. They indicate that $\delta_P - \delta_T$ is mainly determined from a.

Finally the decay-time dependent CP asymmetries expected from one year of data taking with the LHC-B detector are simulated for $|P/T| = 0.2$, $\delta_P - \delta_T = 30°$ and $\alpha = 70°$, $80°$, $90°$, $100°$ and $110°$. The expression given in equation 1 is then fitted to the simulated CP asymmetries where α and $\delta_P - \delta_T$ are treated as free parameters while $|P/T|$ is fixed to 0.2. Figure 4 shows the result of the fit for $\alpha = 110°$ where the most probable values and the one standard deviation contour line is plotted.

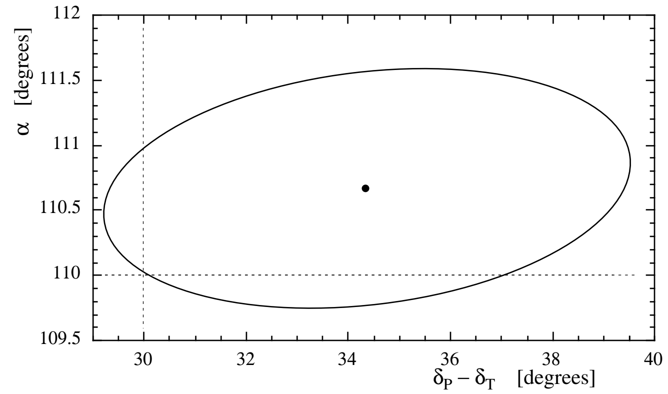

Figure 4: The fitted value of α and $\delta_P - \delta_T$ and the one standard deviation contour line for $\alpha = 110°$, $\delta_P - \delta_T = 30°$ and $|P/T| = 0.2$ where $|P/T|$ is fixed to 0.2 in the fit. One year of data taking with the LHC-B detector is assumed.

Table 2 gives the obtained errors on α and $\delta_P - \delta_T$ and the correlation coefficient between α and $\delta_P - \delta_T$, ρ. The correlation between α and $\delta_P - \delta_T$ is very small. By changing the value of $|P/T|$ by $\pm 10\%$, additional uncertainties of $\pm \sim 1°$ ($\pm \sim 2°$) and $\pm \sim 3°$ ($\pm \sim 4°$) at $\alpha = 70°$ ($\alpha = 110°$) are introduced to α and $\delta_P - \delta_T$ respectively.

Table 2: Errors, σ, and correlation coefficients, ρ, for the measured values of α and $\delta_P - \delta_T$ for $\alpha = 70°$, $80°$, $90°$, $100°$ and $110°$ with $|P/T| = 0.2$ and $\delta_P - \delta_T = 30°$. The value of $|P/T|$ is fixed in the fit. One year of data taking with the LHC-B detector is assumed.

α	70°	80°	90°	100°	110°
σ_α	0.87°	0.87°	0.87°	0.90°	0.95°
$\sigma_{\delta_P - \delta_T}$	6.6°	6.6°	6.1°	5.8°	5.3°
ρ	0.039	0.145	0.106	0.162	0.194

2 The angle γ measurements

Table 3 summarises the expected errors on γ with one year of data taking for $\gamma = 50°$, $70°$ and $90°$ using,

1. $B_s \to D_s^{\pm} K^{\mp}$, assuming $x_s = 20$ and the strong interaction phase difference $\Delta_{D_s K} = 0°$, $10°$ and $30°$;
2. $B_d \to D\,K^{*0}$, assuming the strong interaction phase difference $\Delta_{DK^*} = 0°$, $10°$ and $30°$.

The expected range of γ is from $0°$ to $180°$. However, the $B_d \to D\,K^{*0}$ decay mode is sensitive to $\sin 2\gamma$ and the measured value of γ is restricted the range from $0°$ to $90°$. The angular resolutions

Table 3: Expected errors on γ with one year of data taking for $\gamma = 50°$, $70°$ and $90°$ using two decay modes.

γ	$50°$	$70°$	$90°$	$50°$	$70°$	$90°$	$50°$	$70°$	$90°$
$\Delta_{\mathrm{D_sK}}$	$0°$			$10°$			$30°$		
σ_γ with $\mathrm{B_s} \to \mathrm{D_s^\pm K^\mp}$	$5.9°$	$9.4°$	$16.2°$	$6.0°$	$8.9°$	$14.5°$	$8.1°$	$12.1°$	$7.4°$
$\Delta_{\mathrm{DK^*}}$	$0°$			$10°$			$30°$		
σ_γ with $\mathrm{B_d} \to \mathrm{DK^*}$	$11°$	$12°$	$9.0°$	$11°$	$12°$	$10°$	$7.4°$	$9.0°$	$11°$

for $\gamma = 90°$ are obtained by assuming that the measurement can go beyond $90°$. The γ measured by $\mathrm{B_s} \to \mathrm{D_s^\pm K^\mp}$ does not have this restriction and is sensitive from $\gamma = 0°$ to $180°$. On the other hand, the errors on the measured γ increase by $\sim 35\%$ if x_s is increased to 30. In the standard model, γ decreases when x_s increases.

It should be noted that the strong interaction phase differences can be also determined from the data for both $\mathrm{D_s^\pm K^\mp}$ and $\mathrm{D\,K^{*0}}$. Therefore, no ambiguity is introduced to the measured values of γ by those phase differences. There is no relation between the strong interaction phases of the two decay modes.

Since the two measurements use different decay modes and methods, possible systematic effects can be studied by comparing the two. We can also combine the two results in order to reduce the error on γ.